

Electron Beam Surface Hardening of Gear Teeth

Hartowanie powierzchniowe uzębień kół zębatych wiązką elektronów

Abstract: Surface hardening is an effective method enabling the improvement of the wear resistance of components subjected to friction, without the necessity of hardening the entire component. Because of easy dynamic deflection and focusing as well as due to very high heating rates, the use of electron beam enables the obtainment of layers characterised by suitable properties. The article describes the electron beam surface hardening of gear teeth made of steel 34CrAlNi7-10 (1.8550) as well as discusses metallographic test results and Vickers hardness measurement results demonstrating the effectiveness of the method in the obtainment of layers characterised by uniform thickness and a hardness of 660 HV0.1.

Key words: Electron beam, surface hardening, gear hardening

Streszczenie: Hartowanie powierzchniowe jest skuteczną metodą poprawy odporności na zużycie elementów narażonych na tarcie, bez konieczności hartowania całego elementu. Zastosowanie wiązki elektronów umożliwia uzyskanie warstw o odpowiednich właściwościach, dzięki łatwemu, dynamicznemu odchyłaniu i ogniskowaniu oraz bardzo wysokim szybkościom nagrzewania. W artykule przeprowadzono proces hartowania powierzchniowego uzębień kół zębatych ze stali 34CrAlNi7-10 (1.8550) za pomocą wiązki elektronów. Przeprowadzono badania metalograficzne i pomiar twardości metodą Vickersa, dzięki którym przedstawiono skuteczność tej metody, uzyskując warstwy o równomiernej grubości i twardości rzędu 660 HV0,1.

Słowa kluczowe: wiązka elektronów, hartowanie powierzchniowe, hartowanie kół zębatych

1. Introduction

Presently, methods enabling the surface processing of iron elements are many and varied. One of such methods is surface hardening, involving the heating of the surface layer up to the austenitising temperature followed by fast cooling, aimed at the obtainment of martensite or bainite. The above-named technique reduces stresses and manufacturing costs. Surface hardening, performed with or without melting, includes flame, induction, laser beam-based, electron beam-based, contact and electrolytic hardening methods [1–3].

The use of high-energy fluxes, such as electron and laser beams, in the surface treatment of metals and alloys is an increasingly popular trend in industrial production, aimed to improve physical and mechanical properties. The advantages of the above-named methods over conventional techniques include precise parameter control, small zones subjected to treatment and high input energy density. In addition, the methods induce fast heating and cooling, reaching up to 1010 K/s, thus enabling the performance of efficient hardening processes. Electron beam-based treatment technologies have become precise and efficient surface processing methods, the advantages of

which include short treatment times and precise control over beam parameters. The combination of electron beam-based processing with other techniques, such as thin layer (film) deposition and plasma nitriding, improves material properties and paves the way for new industrial applications [4, 5].

Research on critical conditions as regards the electron beam surface hardening of carbon steels has been summarised by Petrov [5]. The calculation of temperature distribution caused by the oscillation of the high-frequency electron beam necessitated the development of a dedicated numerical model. Numerical simulations revealed that heating and cooling rates minimally affected the power of electron beam, yet they depended significantly on the specimen travel rate, triggering an increase at higher rates. As a result, the effectiveness of electron beam hardening in metals increase along with the travel rate of specimens subjected to the treatment.

Śliwiński et al. [6] subjected blocks made of nanobainitic steel to electron beam surface hardening using various positions of the beam. The simulation was performed using the Finite Element Method and verified by Vickers hardness tests as well as by light and scanning electron microscopy. The results revealed the obtainment of hardened

mgr inż. Paweł Pogorzelski, mgr inż. Piotr Śliwiński, dr inż. Marek St. Węglowski – Łukasiewicz Research Network – Upper Silesian Institute of Technology, Gliwice, Poland

dr hab. inż. Andrzej Wieczorek – Silesian University of Technology, Poland

dr inż. Emilia Skołek – Warsaw University of Technology, Poland

Corresponding Author: pawel.pogorzelski@git.lukasiewicz.gov.pl

layers having a thickness of up to 1.9 mm. The hardness in the hardened zone was uniform, with the specimens hardened without movement characterised by a higher layer mean hardness value of 674 HV0.1. The mean hardness of the specimens hardened at a rate of 250 mm/min amounted to 626 HV0.1. The numerical calculation results were consistent with those obtained experimentally, which demonstrated the accuracy of the electron beam hardening model.

Research conducted by Zhang et al. [7] was concerned with the laser beam hardening of gear wheel surfaces and aimed to solve problems of deformations triggered by laser beam hardening. The research was focused on the implementation of techniques including the adjustment of the motion of gear wheels as well as changes in the rate and the use of cooling. The experiments involved the use of gear wheels made of medium-carbon steel and changes of parameters such as the power and travel rate of the laser beam. The results revealed uniform hardening with little deformations, implying that laser hardening was a viable option enabling the improvement of low-quality gears without compromising precision. The summary emphasized the importance of the procedures in the effective laser hardening of gear wheels, referring to previous research on the laser processing of materials and surface engineering.

Article [8] discussed experiments performed by Śliwiński et al., involving the electron beam surface hardening of shafts made of steel C45. The tests resulted in the obtainment of uniform layers having a thickness of up to 400 µm and a hardness of up to 900 HV0.1.

2. 2. Test and results

2.1. Test materials

The tests involved the use of a gear wheel made of steel 34CrAlNi7-10 (1.8550), the chemical composition of which (in accordance with the PN-EN ISO 683-5:2021-10 standard) is presented in Table 1. The wheel diameter was Ø283 mm, the total height of a tooth amounted to 24.2 mm, whereas the gear tooth module amounted to 10 mm.

Table 1. Chemical composition of steel 34CrAlNi7-10 (1.8550) [9]

Chemical composition [%]								
C	Mn	Si	P	S	Cr	Mo	Ni	Al
0.30–0.37	0.4–0.6	0.15–0.35	<0.025	<0.025	1.5–1.8	0.15–0.25	0.9–1.1	0.8–1.1

2.2. Electron beam hardening

The electron beam surface hardening process was performed using a CVE EB 756 electron beam welding machine (Cambridge Vacuum Engineering), located at the Centre of Welding. The welding machine was provided with a high-voltage generator having a maximum power of 30 kW, a directly heated cathode and the stepless adjustment of accelerating voltage up to 150 kV. Operating pressure in the chamber was restricted within the range of 10⁻⁴ mbar to 10⁻⁵ mbar.

The tests included two methods, where surface processing was performed using a specific oscillation pattern. The first method included beam oscillation and the simultaneous motion along the tooth tip. In turn, the second method involved the use of the beam oscillating in a specific pat-

tern, covering the entire surface subjected to hardening, without moving along the tooth. The above-named hardening methods are presented in Fig. 1. Table 2 contains parameters characteristic of a given hardening test, whereas Table 3 contains oscillation patterns used in the tests. The process parameters, common for all the tests, were the following:

- accelerating voltage – 140 kV
- working distance – 420 mm (set at the half of the tooth height)
- cathode heater current – 22 A
- focusing coil current – 680 mA (debunched beam, where debunched beam current in relation to the above-presented accelerating voltage and working distance amounted to 710 mA)
- beam oscillation frequency – 10 Hz (except for tooth XVII)
- hardening rate – 100 mm/min (only for teeth I–XIII, except for tooth X)
- tungsten cathode width – 2 mm.

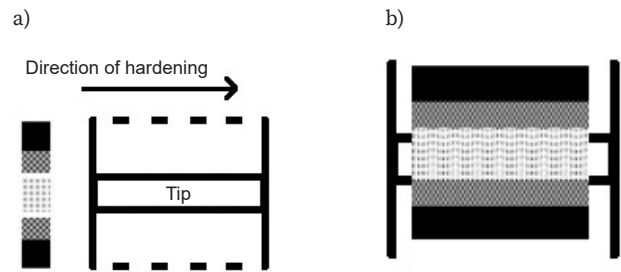
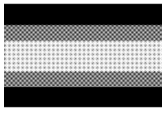
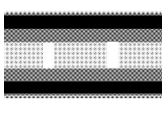
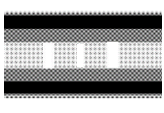


Fig. 1. Hardening methods: a) hardening with oscillation and the simultaneous motion along the tip and b) hardening with the oscillation of the entire tooth, without addition motion

Table 2. Variable parameters used in the hardening tests

Tooth no.	Parameters	Tooth no.	Parameters
I	Pattern A1 I _B = 18 mA	XIV	Pattern B1 I _B = 80 mA t = 4.2 s
II	Pattern A2 I _B = 24 mA	XV	Pattern B2 I _B = 100 mA t = 6 s
III	Pattern A3 I _B = 21 mA	XVI	Pattern B3 I _B = 100 mA t = 4.7 s
IV	Pattern A4 I _B = 19 mA	XVII	Pattern B4 I _B = 70 mA 5 Hz t = 12 s
V	Pattern A5 I _B = 25 mA	XVIII	Pattern B5 I _B = 100 mA t = 9 s
VI	Pattern A6 I _B = 22 mA	XIX	Pattern B6 I _B = 100 mA t = 6.4 s
VII	Pattern A1 I _B = 17 mA	XX	Pattern B7 I _B = 100 mA t = 7.1 s
VIII	Pattern A2 I _B = 20 mA	XXI	Pattern B1 I _B = 80 mA t = 3.5 s
IX	Pattern A3 I _B = 23 mA	XXII	Pattern B2 I _B = 100 mA t = 4.5 s
X	Pattern A3 I _B = 21 mA V = 80 mm/min	XXIII	Pattern B4 I _B = 100 mA t = 8.5 s
XI	Pattern A4 I _B = 21 mA	XXIV	Pattern B7 I _B = 100 mA t = 5 s
XII	Pattern A4 I _B = 19 mA		
XIII	Pattern A4 I _B = 20 mA		

Table 3. Oscillation patterns (darker areas represent areas characterised by more intense beam effect)

Oscillation number	Oscillation pattern	Oscillation number	Oscillation pattern
A1		B1	
A2		B2	
A3		B3	
A4		B4	
A5		B5	
A6		B6	
		B7	

Before hardening, the gear surface was cleaned chemically using acetone. Afterwards, the gear was fixed in a self-centring three-jaw chuck (see Fig. 2). Figure 3 presents selected teeth after heat treatment.

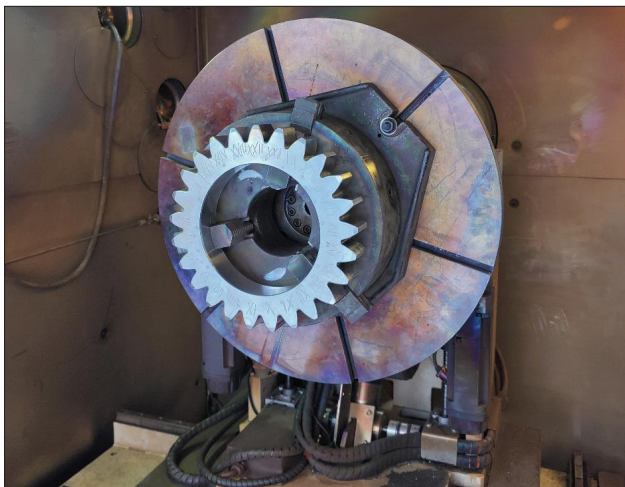


Fig. 2. Gear wheel before hardening

2.3. Metallographic tests

The test specimens were prepared after the hardening process. The metallographic tests were performed using an Eclipse MA200 microscope (Nikon), in accordance with

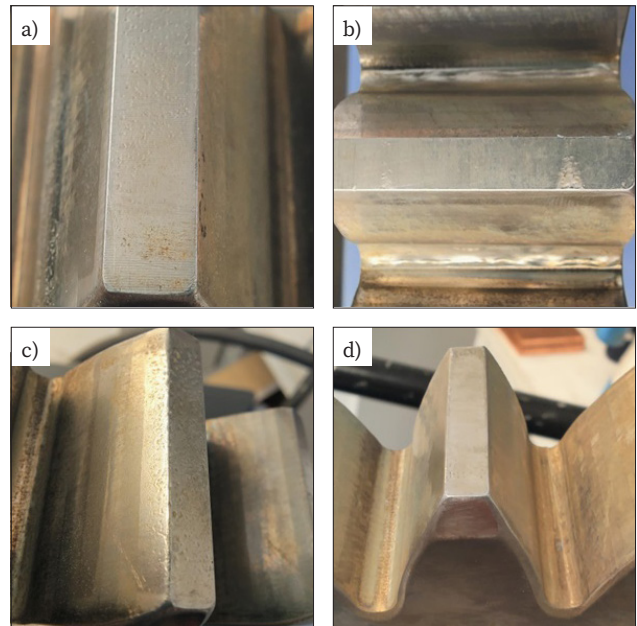


Fig. 3. Selected teeth after hardening: a) tooth II, b) tooth XV, c) tooth IX and d) tooth III

the PN-EN ISO 17639:2022-07 standard [10]. The etchant used to reveal the cross-sectional macrostructure of the teeth was Adler's reagent. In turn, the etchant used to reveal the microstructure was Nital. Figures 4 and 5 present cross-sections of selected teeth, whereas Figure 6 presents the microstructure of the hardened layer, transition layer and the core material of tooth no. II.

2.4. Hardness measurements

The subsequent stage of research involved hardness measurements performed under a load of 0.98 N (HV 0.1), using an automatic hardness tester (Prüftechnik). The tests were performed along three measurement lines, perpendicularly from the tooth surface to the core and along one line parallel to the tooth tip surface. Figure 7 presents the measurement lines. The hardness test results obtained along the measurement lines a, b and c are presented as diagrams in Figures 8 through 10.

3. Discussion

The analysis of the test results revealed that the most uniform thickness of the hardened layers was observed in the specimens subjected to hardening in motion. Particularly uniformly hardened layers were observed in specimen II, whereas the greatest hardening depth was observed in the specimens not subjected to displacement (movement) during the process (particularly specimens XVII and XX).

The microstructural photographs of the tooth presented in Figure 6 revealed the presence of several zones. The area hardened on the side and at the tip of the tooth contained the martensitic structure. The transition zone between the hardened area and the tooth core contained the martensitic-bainitic structure. The tooth core was characterised by the bainitic structure.

The analysis of hardness measurement results presented in Figures 8 through 10 revealed decreasing hardness along with an increasing distance of consecutive measurement readouts from the tooth surface, indicating the proper

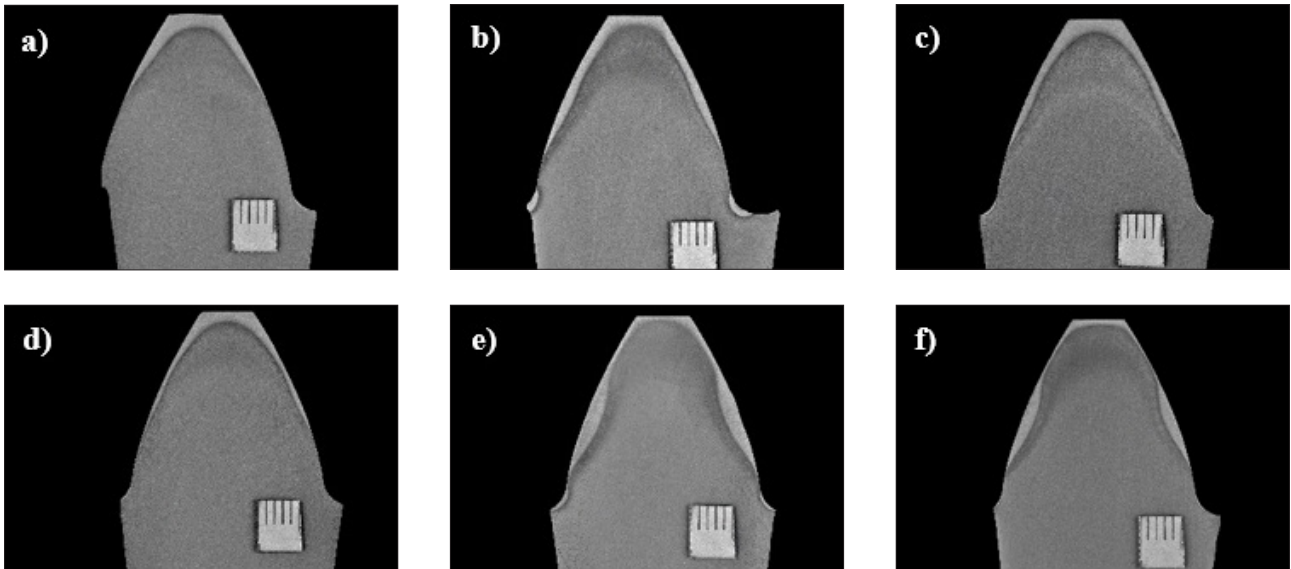


Fig. 4. Cross-sections of selected teeth: a) tooth I, b) tooth II, c) tooth III, d) tooth IV, e) tooth V and f) tooth VI

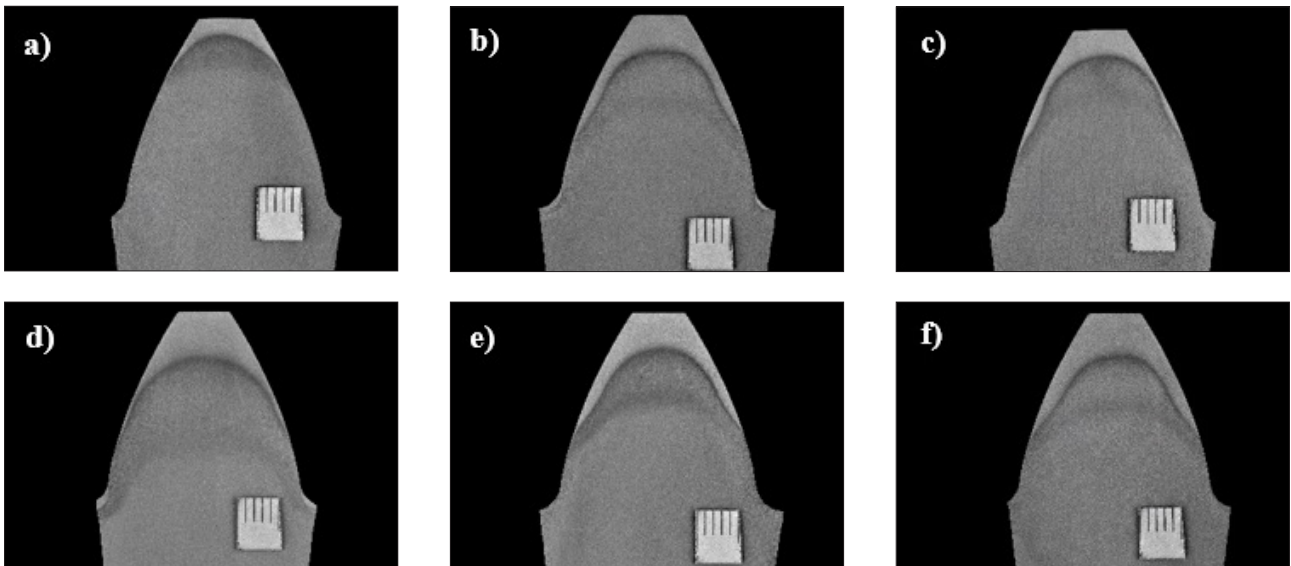


Fig. 5. Cross-sections of selected teeth: a) tooth XIV, b) tooth XV, c) tooth XVI, d) tooth XVII, e) tooth XIX and f) tooth XX

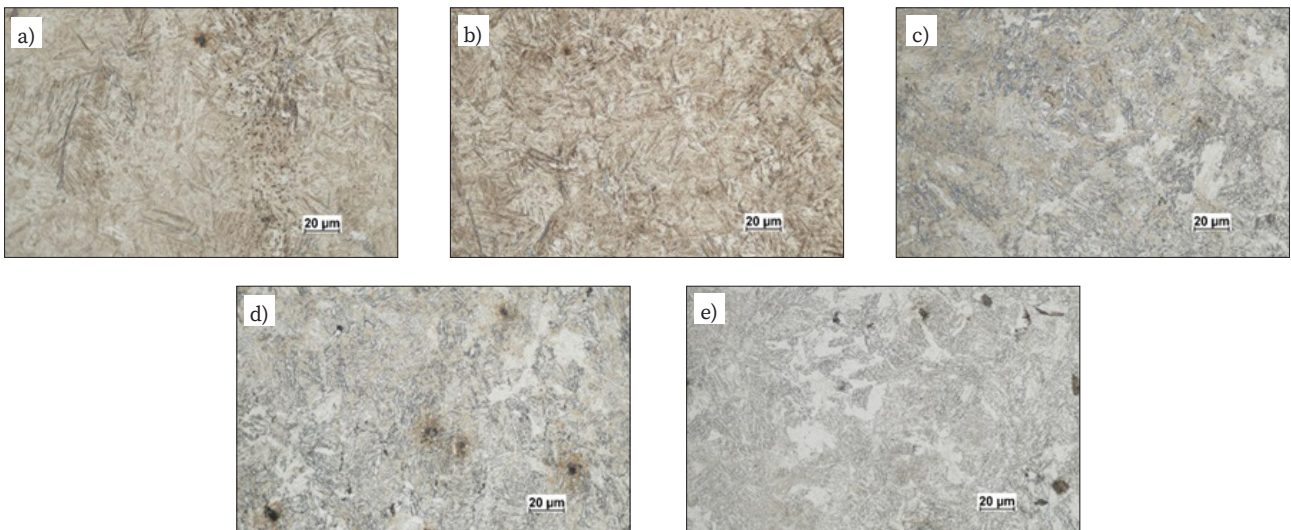


Fig. 6. Microstructure of tooth II: a) hardened layer on the tooth side, b) hardened layer at the tooth tip, c) transition layer on the tooth side, d) transition layer at the tooth tip and e) tooth core material

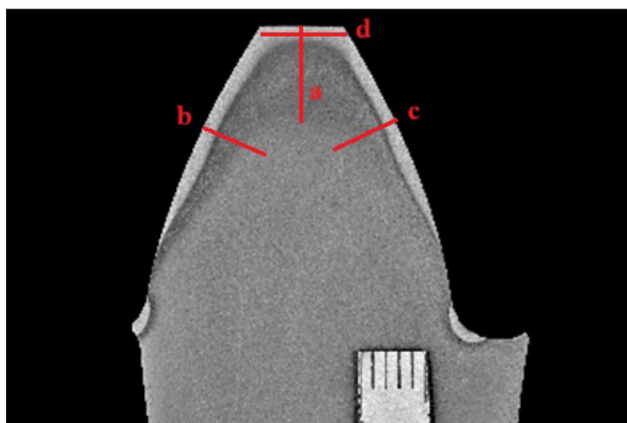


Fig. 7. Measurement lines in the hardness tests

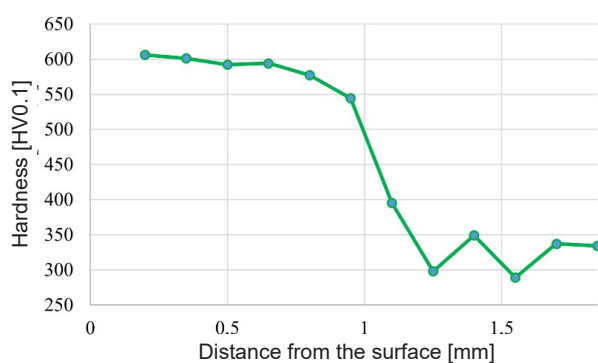


Fig. 8. Hardness distribution in the direction perpendicular to the tooth tip surface – line a

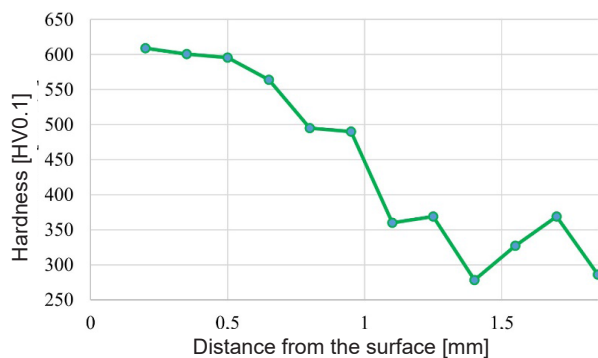


Fig. 9. Hardness distribution in the direction perpendicular to the tooth side surface – line b

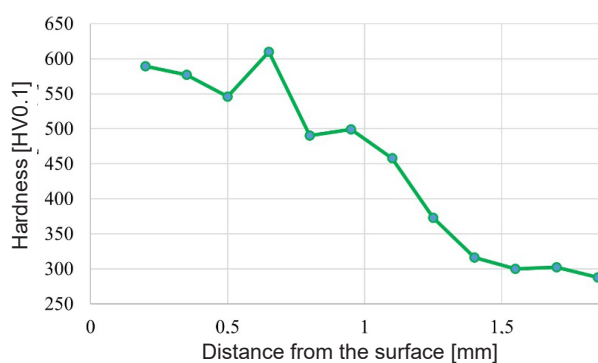


Fig. 10. Hardness distribution in the direction perpendicular to the tooth side surface – line c

performance of the process. The measurement results obtained along the measurement line parallel to the surface (line d) enabled the determination of the mean hardness of the hardened layer amounting to 660 HV0.1; the standard deviation being 44 HV0.1.

4. Conclusions

The above-presented tests and results led to the formulation of the following conclusions:

1. The electron beam hardening method discussed in the research work enabled the obtainment of a uniformly hardened layer across most of the cross-section of the test gear tooth.
2. The hardening process made it possible to increase the hardness of the material restricted within the range of 300 HV0.1 to 350 HV0.1 to a mean hardness of 660 HV0.1.
3. Because of electron beam sensitivity to the angle of incidence (on the workpiece material) it was not possible to entirely harden the side surface of the tooth at its root. The prevention of the foregoing requires the performance of tests changing the beam angle of incidence so that the beam could vertically strike the notch bottom instead of the tooth tip. Another solution could involve the performance of the hardening process involving the use of oscillation with the simultaneous rotation of the gear (aimed to eliminate the unfavourable beam angle of incidence).

Article submitted to the 28th Scientific and Technical National Welding Conference "Progress, innovations and quality requirements of welding processes" (Międzyzdroje, 21-23.05.2024 r.)

REFERENCES

- [1] Śliwiński P., Węglowski M.S., Kwieciński K., Wieczorek A.: Electron beam surface hardening. *Biuletyn Instytutu Spawalnictwa*, 2022, vol. 66, no. 1, pp. 7-20.
- [2] Vanapaemel J.: History of the hardening of steel: science and technology. *Journal de Physique Colloques*, 1982, vol. 43, no. C4, pp. C4-847-C4-854.
- [3] Rudnev V.: Induction Hardening of Gears and Critical Components. *Gear technology*. 2008, wrzesień/październik, pp. 58-63, www.geartechnology.com.
- [4] Valkov S., Ormanova M., Petrov P.: Electron-Beam Surface Treatment of Metals and Alloys. *Techniques and Trends. Metals 2020*, vol. 10, no. 9, art. no. 1219.
- [5] Petrov P.: Optimization of carbon steel electron-beam hardening. *Journal of Physics: Conference Series*, 2010, 223 012029.
- [6] Śliwiński P., Węglowski M.S., Pikuła J., Tański T., Wieczorek A.N., Skolek E.: Electron beam hardening of nanobainitic steels. *Biuletyn Instytutu Spawalnictwa*, 2023, vol. 67, no. 2, pp. 24-37.
- [7] Zhang H., Shi Y., Xu C.Y., Kutsuna M.: Surface Hardening of Gears by Laser Beam Processing. *Surface Engineering*. 2003, vol. 19, no. 2, pp. 134-136.
- [8] Śliwiński P., Kubik K., Kopyściański M.: Electron beam Surface hardening of steel C45. *Biuletyn Instytutu Spawalnictwa*, 2022, vol. 66, no. 6, pp. 27-35.
- [9] PN-EN ISO 683-5:2021-10. Stale do obróbki cieplnej, stale stopowe i stale automatowe – Część 5: Stale do azotowania.
- [10] PN-EN ISO 17639:2022-07. Badania niszczące spawanych złączy metali – Badania makroskopowe i mikroskopowe złączy spawanych.